BEST AVAILABLE IMAGES

Defective images within this document are accurate representations of the original documents submitted by the applicant.

Defects in the images may include (but are not limited to):

- BLACK BORDERS
- TEXT CUT OFF AT TOP, BOTTOM OR SIDES
- FADED TEXT
- ILLEGIBLE TEXT
- SKEWED/SLANTED IMAGES
- COLORED PHOTOS
- BLACK OR VERY BLACK AND WHITE DARK PHOTOS
- GRAY SCALE DOCUMENTS

IMAGES ARE BEST AVAILABLE COPY.

As rescanning documents *will not* correct images, please do not report the images to the Image Problem Mailbox.

REMARKS

Claim 34 has been cancelled thus rendering moot the objection to that claim under 37 CFR 1.75(c).

Claim 1 has been amended to clarify that the alloy is cooled to 0° by quenching in ice water in step (4).

The non-statutory double patenting rejection is noted. Applicants will file a Terminal Disclaimer once the application is otherwise indicated to be allowable.

Turning to the art rejection, the Examiner acknowledges the claims are novel; however, the Examiner takes the position that the claims are obvious from the art. In this regard, it is noted the Examiner acknowledges in rejecting claims 22, 23, 26-28, 31, 32, 34 and 37-39 as being obvious over JP '180 that the applied art does not disclose repeatedly melting and solidifying. However, the Examiner takes the position that the claimed two step combination is obvious. Actually, independent claim 22 has other distinguishing features. For example, independent claim 22 requires that the alloy is rapidly cooled to 0°C by quenching in the ice water. Contrary to the Examiner's assertion in the second full paragraph under "Response to Arguments" on page 6 of the Action, quenching in iced water is not the same as quenching in water. When hot (high temperature) materials are rapidly quenched in iced water, the temperature of the quenching liquid is maintained at 0°C until the ice is completely melted. In contrast, when quenching in water, the temperature of the liquid rapidly rises since the cooling power of water, i.e., the heat capacity of water is significantly less than that of iced water since the heat capacity of ice is significantly more than the heat capacity of water per se.

Further with regard to the foregoing, and with reference to the third paragraph under "Response to Arguments" on page 6 of the Action, the Examiner states "...the BCC intensity

HAYES SOLOWAY P.C.
130 W. CUSHING STREET
TUCSON, AZ 85701
TEL. 520.882.7623
FAX. 520.882.7643

175 CANAL STREET
MANCHESTER, NH 03101
TEL. 603.668.1400
FAX. 603.668.8567

from oil quenching is many times stronger than intensity due to iced-water quenching. Furthermore, as compare BCC intensity to C15 and C36 laves intensities that C15 and C36 laves intensities are appeared as noise level."

The Examiner's statements are in error

In general, samples rapidly cooled with a strong cooling power contain fine crystal grains and strains induced by rapid cooling. Such fine crystal grains and strains weaken X-ray diffraction intensities (see B. D. Cullity, Elements of X-Ray Diffraction, pp. 264-265, Addison-Wesley Publishing Co., Inc., Appendix 1).

With oil-quenched samples, the cooling speed is quite slow, leading to the growth of crystal grains and the alleviation of strains. Accordingly, the BCC peak from oil quenching becomes higher.

Iced-water quenched alloys made in accordance with the present invention essentially have only the BCC phase while the oil quenched one is contaminated with the C15 and C36 laves. And in the case of Applicants' claimed invention a BCC monophase alloy is formed substantially free of laves phases.

In the paragraph bridging pages 6-7 of the Action, the Examiner takes the position that at the plateus hydrogen gas pressure of 0.4, iced-water quenched sample has less protium concentration than oil quenched samples. Again, the Examiner is in error. Referring to Graph 2, (Appendix 3) black marks (●, ▲ and ■) refer to a process of absorbing hydrogen and white marks (○, △ and □) refer to a process of releasing hydrogen.

In general, a material is usually employed as a hydrogen storage alloy within the pressures ranging from 0.1 MPa (about 1 atm) to the upper limit, 10 MPa (about 100 atm). For example, when used for powering motor vehicles, the applicable pressure range is from about

HAYES SOLOWAY P.C.
130 W. CUSHING STREET
TUCSON, AZ 85701
TEL. 520.882.7623
FAX. 520.882.7643

175 CANAL STREET
MANCHESTER, NH 03101
TEL. 603.668.1400
FAX. 603.668.8567

0.1 MPa (about 1 atm) to about 1 MPa (about 10 atm) (by referring to Graph 2, for example, the generally utilizable hydrogen pressure range is from about 0.08 MPa to about 1.0 MPa). It should be noted that, for hydrogen storage applications, the hydrogen-releasing process represented by white marks (○, △ and □) is important.

In Graph 2, the plateau ranges from nearly 3.35% to nearly 1.15% for Sample △ (quenched in iced water). This means that the released hydrogen amount of 2.2 % is achievable in this iced-water quenched sample (3.35% - 1.15% = 2.2%).

In contrast, that ranges nearly from 2.85% to 1.3% for Sample □ (quenched in oil). This means that the released hydrogen amount of about 1.55% only is achievable in this oil quenched sample (2.85% - 1.3% = 1.55%).

Thus, it is apparent that the utilizable hydrogen amount of iced-water quenched alloy sample is greater than that of oil quenched alloy sample.

It should be noted that the difference of only 0.2 or 0.3% is incredible in this art field. Thus, the difference, 0.65%, is an unexpectedly superior value.

In actual applications, the pressures at or below 1 MPa (10 atm) are applied. Accordingly, stored hydrogen can be used from the point at about 3.35% for the iced-water quenched sample while from the point at about 2.85% for the oil quenched sample. Thus, the iced-water quenched sample is quite advantageous.

In the paragraph bridging pages 6-7 of the Action, the Examiner also states "At the extreme high hydrogen gas pressures, all sample converge to the same protium concentration." Again the Examiner is in error.

HAYES SOLOWAY P.C.
130 W. CUSHING STREET
TUCSON, AZ 85701
TEL. 520.882.7623
FAX. 520.882.7643

175 CANAL STREET
MANCHESTER, NH 03101
TEL. 603.668.1400
FAX. 603.668.8567

The important measure is not ultimate storage capacity, but rather released hydrogen amount (represented by the white marks in Graph 2).

Therefore, the utilizable hydrogen quantity of iced-water quenched BCC monophase sample is significantly larger than that of oil quenched sample.

In the paragraph in the middle of page 7 of the Action, the Examiner states: "But, Figures 9 and 10 have shown no Mo and W would have the same effect. Moreover, assuming arguendo that the Figures 9 and 10 have shown Mo and W, but the ranges are not consistent with the instant claims."

For Ti-Cr binary alloys wherein no Mo and W is admixed, the limit is a hydrogen absorption capacity of 2.6 mass %, which value the present inventors have been the first to achieve by means of the sophisticated production methods of the present invention. When Mo or W is admixed at 2%, the hydrogen absorption capacity is increased due to the formation of only the BCC phase. Thus, the additive amount at which only the BCC phase can be formed gives a maximum hydrogen absorption capacity.

The reason why the hydrogen absorption capacity (mass%) of W-admixed sample is less than that of Mo-admixed sample among alloys with the same BCC monophase structure is that the atomic weight of W is 183.36, which is far greater (heavier) than that of Mo, 95.95.

In Figures 9 and 10, each hydrogen absorption capacity value is expressed by mass %. Therefore, when an amount of admixed heavy metal W increases, it is natural that such values (mass %) lessen.

As shown in Fig. 1 of Journal of Alloys and Compounds, 356-357 (2003), pp.447-451, (Appendix 2), when each hydrogen absorption capacity value is expressed by H/M (molecular weight), the value is constant from 2% to 10% Mo contents.

HAYES SOLOWAY P.C.
130 W. CUSHING STREET
TUCSON, AZ 85701
TEL. 520.882.7623
FAX. 520.882.7643

175 CANAL STREET
MANCHESTER, NH 03101
TEL. 603.668.1400
FAX. 603.668.8567

Since each hydrogen absorption capacity value is expressed by mass % in Figure 9 and Mo has the heavy atomic weight, even when the same hydrogen amount is absorbed up to 10% Mo content, it appears as if the value decreased.

With regard to the Examiner's comments in the paragraph bridging pages 7-8 of the Action, and the first full paragraph on page 8, it is submitted there is nothing inconsistent. Ideally, the most preferable heat-treating period is about 1 minute. The reason is that Ti is quite likely to be oxidized in Ti-Cr based alloys. Even under inert gas (such as Ar) atmosphere conditions, Ti may react with trace amounts of oxygen, leading to the oxidation of Ti.

In view of practical hydrogen storage alloy applications, up to 2 hours heat-treating period is acceptable because the hydrogen storage capacity is not much changed (reduced). In other words, the maximum storage capacity value, about 3.4, is still incredible and greatly advantageous for Ti-Cr based alloys over the prior art. The desorbed hydrogen amount value, 2.34, is also unexpectedly superior to those in the prior art Ti-Cr based alloys.

It is clearly seen from Graph 4 that the 2 hours' heat-treatment is acceptable.

In the paragraph bridging pages 5-6 of the Action, the Examiner states "With respect to claim 30, that the claimed 8 atomic % is not considered different from 9 atomic % as taught by JP 11-106859 because it is well settled that a prima facie case of obviousness would exist where the claimed ranges and prior art do not overlap but are close enough that one ordinary skilled in the art would have expected them to have the same properties, . . ." (underlining added for emphasis).

The Examiner is in error. In the prior art, it was impossible to produce an alloy with a hydrogen storage capacity of at least 2.6 mass % or more even when a level of constituent element V contained in the alloy mixture is greatly reduced to less than 10 at % (i.e., nearly

HAYES SOLOWAY P.C.
130 W. CUSHING STREET
TUCSON, AZ 85701
TEL. 520.882.7623
FAX. 520.882.7643

175 CANAL STREET
MANCHESTER, NH 03101
TEL. 603.668.1400
FAX. 603.668.8567

zero levels). Simply put there are no reported data and no documents reporting such unexpected experimental data with regard to such extremely-low V level alloys in the prior art.

In contrast, because of unexpectedly and sophisticated production steps of the present invention, the present inventors have succeeded in producing alloys with an increasing high hydrogen storage capacity level even when the V level is reduced to nearly 9 at % or less. It should be noted that the upper limit of the hydrogen storage capacity levels obtained in the prior art JP 11-106859 is merely 1.38 H/M and the lowest level of constituent V in the prior art actually disclosed example alloys with data is 19.0 at % (in JP 11-106859, the fourth constituent element is essential).

(i) It is apparent that it was impossible to reduce the V level to a zero value or a value close thereto while maintaining or increasing the high hydrogen storage capacity in the prior art.

(ii) Within the claimed ranges of V, Mo, or W levels, the present invention provides alloys with an excellently high hydrogen storage capacity, supported by data. The hydrogen absorption capacity level of 2.6 mass% or higher is incredible for Ti-Cr based alloys over the prior art.

The present inventors are the first to achieve such superior performance for significantly-low V, Mo, or W level hydrogen storage Ti-Cr based alloys in the world.

Quite apart from the foregoing, the Examiner should be aware one of the inventors, Dr. Masuo Okada, is considered to be one of the world's experts in materials science, particularly in the field of hydrogen absorbing materials (See Appendix 4).

Accordingly, the rejection of the claims as obvious from the art is in error.

HAYES SOLOWAY P.C.
130 W. CUSHING STREET
TUCSON, AZ 85701
TEL. 520.882.7623
FAX. 520.882.7643

175 CANAL STREET
MANCHESTER, NH 03101
TEL. 603.668.1400
FAX. 603.668.8567

The foregoing amendment makes no claim changes that would require further search by the Examiner. Accordingly, entry of the foregoing amendment, and allowance of the application are respectfully requested.

Having dealt with all the objections raised by the Examiner, the Application is believed to be in order for allowance. Early and favorable action are respectfully requested.

In the event there are any fee deficiencies or additional fees are payable, please charge them (or credit any overpayment) to our Deposit Account No. 08-1391.

Respectfully submitted,

Norman P. Soloway
Attorney for Applicants
Reg. No. 24,315

CERTIFICATE OF TRANSMISSION VIA FACSIMILE

I hereby certify that this correspondence is being sent via facsimile to EXAMINER Sikyin Ip of the United States Patent and Trademark Office at facsimile number (703) 872-9306, on June 28, 2004, 2004 from Tucson, Arizona.

By _____

NPS:sb

HAYES SOLOWAY P.C.
130 W. CUSHING STREET
TUCSON, AZ 85701
TEL. 520.882.7623
FAX. 520.882.7643

175 CANAL STREET
MANCHESTER, NH 03101
TEL. 603.668.1400
FAX. 603.668.8567

APPENDIX 1

ELEMENTS OF
X-RAY DIFFRACTION

by
B. D. CULLITY
Department of Metallurgical Engineering
and Materials Science
University of Notre Dame

ADDISON-WESLEY PUBLISHING COMPANY, INC.
READING, MASSACHUSETTS · PALO ALTO · LONDON · DON MILLS, ONTARIO

stress. (Such stress is often called "internal stress" but the term is not very informative since all stresses, residual or externally imposed, are internal. The term "residual stress" emphasizes the fact that the stress remains after all external forces are removed.) Stresses of this kind are also called *microstresses* since they vary from one grain to another, or from one part of a grain to another part, on a microscopic scale. On the other hand, the stress may be quite uniform over large distances; it is then referred to as *macrostress.*

The effect of strain, both uniform and nonuniform, on the direction of x-ray reflection is illustrated in Fig. 9-2. A portion of an unstrained grain appears in (a) on the left, and the set of transverse reflecting planes shown has everywhere its equilibrium spacing d_0. The diffraction line from these planes appears on the right. If the grain is then given a uniform tensile strain at right angles to the reflecting planes, their spacing becomes larger than d_0, and the corresponding diffraction line shifts to lower angles but does not otherwise change, as shown in (b). This line shift is the basis of the x-ray method for the measurement of macrostress, as will be described in Chap. 17. In (c) the grain is bent and the strain is nonuniform; on the top (tension) side the plane spacing exceeds d_0, on the bottom (compression) side it is less than d_0, and somewhere in between it equals d_0. We may imagine this grain to be composed of a number of small regions in each of which the plane spacing is substantially constant but different from the spacing in adjoining regions. These regions cause the various sharp diffraction lines indicated on the right of (c) by the dotted curves. The sum of these sharp lines, each slightly displaced from the other, is the broadened diffraction line shown by the full curve and, of course, the broadened line is the only one experimentally observable. We can find a relation between the broadening produced and the nonuniformity of the strain by differentiating the Bragg law. We obtain

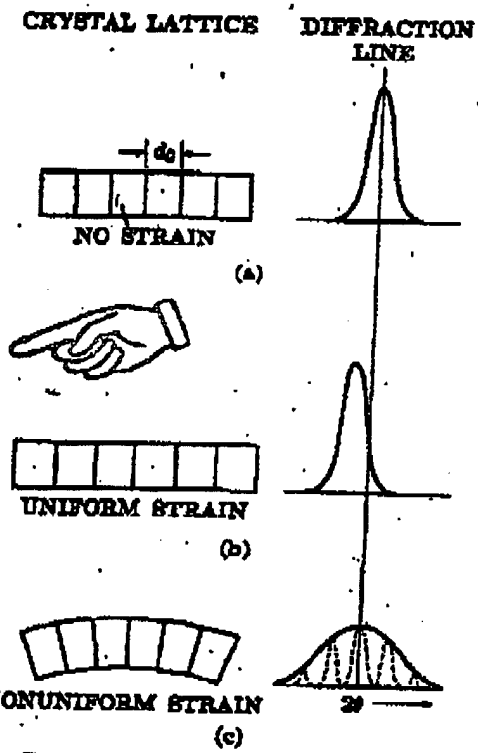

FIG. 9-2. Effect of lattice strain on Debye-line width and position.

$$b = \Delta 2\theta = -2\frac{\Delta d}{d}\tan\theta, \qquad (9\text{-}2)$$

where δ is the broadening due to a fractional variation in plane spacing $\Delta d/d$. This equation allows the variation in strain, $\Delta d/d$, to be calculated from the observed broadening. This value of $\Delta d/d$, however, includes both tensile and compressive strain and must be divided by two to obtain the maximum tensile strain alone, or maximum compressive strain alone, if these two are assumed equal. The maximum strain so found can then be multiplied by the elastic modulus E to give the maximum stress present. For example,

$$(\text{Max. tens. stress}) = E \cdot (\text{max. tens. strain}) = (E)\left(\tfrac{1}{2}\right)\left(\frac{\Delta d}{d}\right) = \frac{Eb}{4 \tan \theta}.$$

When an annealed metal or alloy is cold worked, its diffraction lines become broader. This is a well-established, easily verified experimental fact, but its explanation has been a matter of controversy. Some investigators have felt that the chief effect of cold work is to fragment the grains to a point where their small size alone is sufficient to account for all the observed broadening. Others have concluded that the nonuniformity of strain produced by cold work is the major cause of broadening, with grain fragmentation possibly a minor contributing cause. Actually, it is impossible to generalize, inasmuch as different metals and alloys may behave quite differently. By advanced methods of mathematical analysis, it is possible to divide the observed change in line shape produced by cold work into two parts, one due to fine particle size and the other due to nonuniform strain. When this is done, it is found, for example, that in alpha brass containing 30 percent zinc the observed broadening is due almost entirely to nonuniform strain, while in thoriated tungsten (tungsten containing 0.75 percent thorium oxide) it is due both to nonuniform strain and fine particle size. But no example is known where all the observed broadening can be ascribed to fine particle size. In fact, it is difficult to imagine how cold work could fragment the grains to the degree necessary to cause particle-size broadening without at the same time introducing nonuniform strains, in view of the very complex forces that must act on any one grain of an aggregate no matter how simple the forces applied to the aggregate as a whole.

The broadening of a diffraction line by cold work cannot always be observed by simple inspection of a photograph unless some standard is available for comparison. However, the separation of the $K\alpha$ doublet furnishes a very good "internal standard." In the back-reflection region, an annealed metal produces a well-resolved doublet, one component due to $K\alpha_1$ radiation and the other to $K\alpha_2$. For a given set of experimental conditions, the separation of this doublet on the film is constant and independent of the amount of cold work. But as the amount of cold work is increased, the broadening increases, until finally the two components

APPENDIX 2

ELSEVIER

Journal of Alloys and Compounds 356–357 (2003) 447–451

Journal of ALLOYS AND COMPOUNDS

www.elsevier.com/locate/jallcom

Protium absorption–desorption properties of Ti–Cr–Mo bcc solid solution alloys

A. Kamegawa*, T. Tamura, H. Takamura, M. Okada

Department of Materials Science, Graduate School of Engineering, Tohoku University, Sendai 980-8579, Japan

Received 10 June 2002; accepted 25 October 2002

Abstract

We have investigated the protium absorption–desorption properties of Ti–Cr–Mo alloys of varying composition, including cycling-induced effects. The capacity of alloys with less than 10 at% Mo has an H/M ratio of 1.8 at 10 MPa hydrogen pressure, and remains almost unchanged regardless of Mo content. The 40Ti–Cr–2.5Mo alloy has the widest plateau region observed in this study. The amount of protium desorption and the mean particle size vary inversely with the logarithm of cycle number up to 300 cycles. The capacity of the alloy is drastically affected by the conditions of cycling. With longer evacuation times the capacity decreases significantly. The lattice parameter of the β protide increases with increasing cycles, and the reflection peaks in XRD studies are broadened. The reduction in capacity after several absorption–desorption cycles is somewhat restored by annealing at 673 K for 2 h under vacuum. The absorption pressure of the plateau for the 101st cycle, after annealing following the 100th cycle, recovers to that of the plateau for the first cycle, but then decreases with additional cycling.

Keywords: Body centered cubic; Solid solution alloys; Hydrogen storage alloy; Protium; PCT isotherm

1. Introduction

Recent interest in hydrogen fuel cell power for emission-free vehicles has driven the investigation of high capacity protium absorbing alloys for hydrogen storage. The use of such alloys offers several advantages, including compactness, safety, and freedom from shape constraints. A likely candidate for the purpose is a Ti- or V-based solid solution alloy with a body centered cubic (bcc) structure.

Vanadium [1] or V-based solid-solutions with a bcc structure are known to absorb about 3.8 mass% (H/M~2) of protium (hydrogen atom) around ambient temperature. Iba and Akiba [2–4] reported that multi-phase Ti–V–Mn alloys consisting of Laves and bcc solid-solution phases had good desorption capacities of nearly 2.1 mass% H. Iba and Akiba [2,5] also reported that a Ti–40at%V–35at%Cr alloy with a bcc structure could desorb about 2.4 mass% protium. We have investigated varying compositions and heat-treatment conditions to increase the protium capacities of Ti–Cr–V alloys [6–19]. The optimum heat-treatment conditions for this alloy were reported to be annealing at 1573 K for 1 min, followed by quenching in water. Okada et al. [6] reported that the Ti–Cr–V alloys with low V content (5–7.5 at% V) yield a high capacity of nearly 3 mass% protium, which is the highest value reported so far at 313 K. The optimum composition of the Ti–Cr–V alloys was also discussed and the alloys with Ti/Cr ratio of 2/3 have a plateau region in their PCT curve around 0.1 MPa (1 atm) with the highest capacity at 313 K. These alloys are promising since they contain a relatively low amount of expensive vanadium. Since the bcc alloys with low V content exhibit high capacities comparable to pure vanadium or V-based alloys, we surmised that V-free Ti–Cr alloys with a bcc structure might also exhibit a high capacity. The equilibrium phase of the Ti–Cr system has a bcc solid-solution in a high and narrow range below the congruent melting point. Therefore, it is difficult to obtain only bcc phase freezing from high temperature in the binary alloys. Recently, we reported that the addition of Mo to Ti–Cr alloys stabilizes the bcc phase in the binary phase diagram, and that adding Mo to Ti–Cr alloys gives

* Corresponding author.
E-mail address: kamegawa@material.tohoku.ac.jp (A. Kamegawa).

0925-8388/02/$ – see front matter
PII: S0925-8388(02)01259-2

not only flattened plateau regions, but also capacities of 3.6 mass% protium similar to Ti–Cr–V alloys [14].

Here we report the protium absorption–desorption properties of Ti–Cr–Mo alloys with varying Mo content and Ti/Cr ratio. The cyclic properties of the alloys are also investigated.

2. Experimental procedures

The alloys were prepared from raw materials by arc melting on a water-cooled copper hearth under pure argon. The purity of the elements was as follows: Ti>99.6 at% and Cr, Mo>99.99 at%. In our previous study, the Ti–Cr–V alloys with added Mo were mainly bcc phase. However, Mo or unmelted additives tended to remain in the alloys with more than 10% Mo, because of molybdenum's comparatively high melting point (2883 K). Therefore, Cr–Mo alloys were melted first, and then Ti–Cr–Mo alloys were prepared. Sample ingots were remelted three times to ensure their homogeneity. To obtain the bcc phase in the alloys and enhance their homogeneity, the samples were annealed at 1673 K for 1 min, and quenched in ice water.

Crystal structures and lattice parameters were studied with an X-ray diffractometer (XRD), using Cu Kα radiation. PCT curves were measured with a Sieverts-type apparatus at 313 K. Each sample was put into a vessel and was evacuated at 313 K for 2 h, using a rotary vacuum pump. The alloys absorb protium fully at the first hydrogen charge process, so initial activation treatments were unnecessary. Hydrogen was introduced gradually into the vessel up to a pressure of 10 MPa. Accelerated cyclic experiments were carried out by holding the sample for 30 min at 10 MPa H_2, followed by evacuation for 1 or 30 min. The evacuation for 30 and 1 min correspond to reducing the hydrogen equilibrium pressure to less than 0.001 and 0.07 MPa, respectively, and were called 'cycle A' and 'cycle B', respectively. The mean particle size of the powder samples after the cyclic experiments was measured with a laser diffraction particle size analyzer.

3. Results and discussion

Fig. 1 shows PCT curves of Ti–(60−*x*)Cr–*x*Mo heat-treated alloys (*x*=2.5, 5, 10, 20, 30, 50). XRD shows only the bcc phase. The pressure of the plateau for these alloys increases with increasing Mo content. The H/M ratio of the alloy with less than 10 at% Mo is as high as 1.8 at 10 MPa hydrogen pressure and does not vary with Mo content. However, the H/M ratio of the alloy with more than 20 at% Mo decreases with increasing Mo content, and the slope of the plateau increases. Furthermore, the mass concentration of absorbed protium decreases with increasing Mo content. The mass absorbing capacity rises to a maximum value of 3.6 mass% when the Mo content is 2.5% Mo, and then decreases with increasing Mo content.

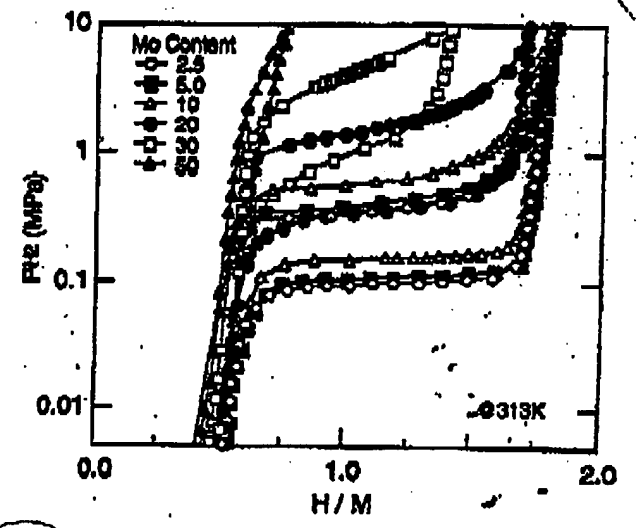

Fig. 1. PCT curves of Ti–(60−*x*)Cr–*x*Mo alloys (*x*=2.5, 5, 10, 20, 30, 50).

Fig. 2 shows PCT curves of *x*Ti–Cr–2.5Mo alloys (*x*=37, 39, 40, 41, 43). XRD showed that alloys with more than 39% Ti consist mainly of the bcc phase, but the 37% Ti alloy contains the bcc phase as a major phase and Laves phase as a minor one, which is known to absorb a small amount of protium at around room temperature. Alloys containing more than 40% Ti absorb protium up to an H/M of 1.8, but the capacities of the alloys with less than 39% Ti decrease with decreasing Ti content. The plateau pressures of the alloys decrease with increasing Ti content, and the 40Ti–Cr–2.5Mo alloy has the widest plateau region in this study.

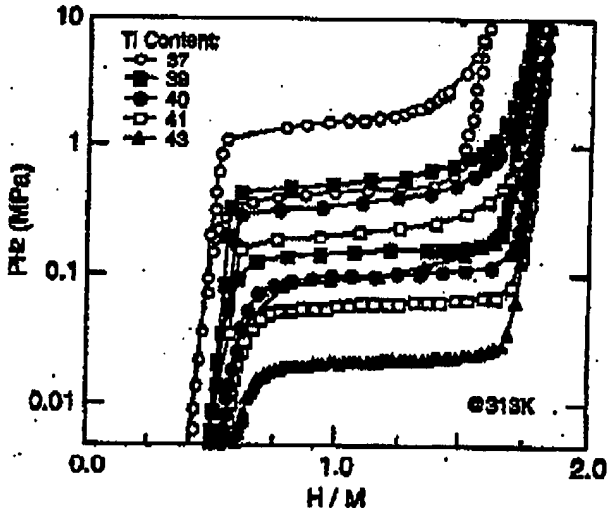

Fig. 2. PCT curves of *x*Ti–(60−*x*)Cr–2.5Mo alloys process (*x*=37, 39, 40, 41, 43).

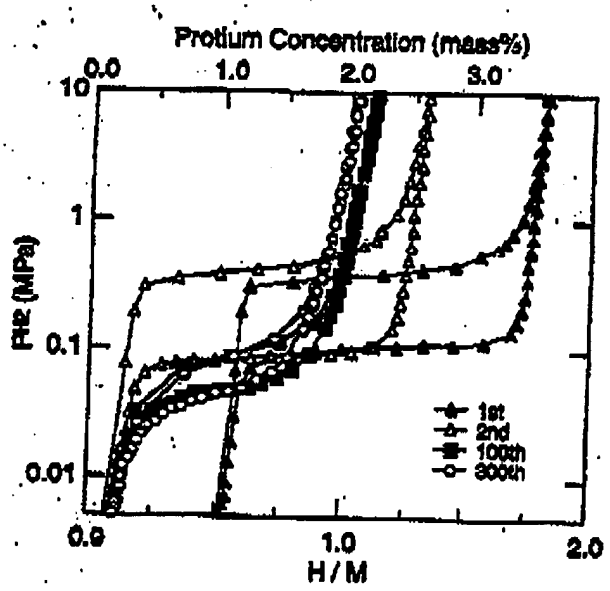

Fig. 3. PCT curves of 40Ti–Cr–2.5Mo alloys for the first, second, 100th, and 300th cycles of Cycle A (10 MPa H_2 for 30 min, then evacuation for 30 min before each measurement).

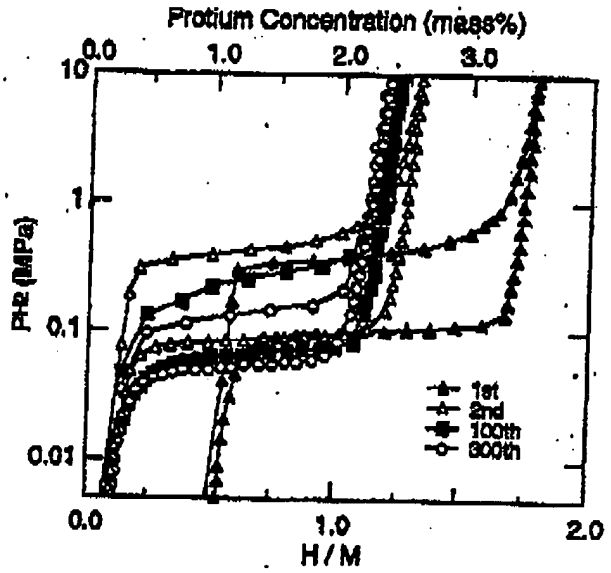

Fig. 4. PCT curves of 40Ti–Cr–2.5Mo alloys for the first, second, 100th, and 300th cycles of Cycle B (10 MPa H_2 for 30 min, then evacuation for 1 min before each measurement).

Fig. 3 shows PCT curves of the 40Ti–Cr–2.5Mo alloy for the first to 300th cycle of cycle A (with a thorough desorbing stage). The reason for the large difference of reversible capacities between PCT curves for the first and second cycle is the resetting of the origin of the protium concentration before the second cycle measurement. While the desorption pressure of the plateau decreases slightly from the first to second cycle, the absorption pressure increases significantly. This phenomenon was also observed for the other alloys in this study. However, both the plateau pressure of the alloy and the reversible capacity decrease drastically beyond the second cycle, with a reduction from an H/M of 1.3 for the second cycle to 1.0 for the 300th cycle. The hysteresis of the curve becomes smaller as the number of cycles increases.

Fig. 4 shows PCT curves of 40Ti–Cr–2.5Mo alloy after undergoing cycle B, with its comparatively smaller desorbing process. Compared with the results in Fig. 3, the decrease in plateau pressure is small and the reversible capacity is large. Although the slope of the desorption plateau does not depend to any significant degree on the number of cycles, the plateau region of the absorption curve declines slightly. The protium concentration of β protide after the absorption–desorption process of cycle B is larger than the concentration after cycle A, as mentioned above. The difference after cycle A and cycle B is the amount of protium in β protide, and the lattice parameter of β protide after cycle A is smaller than that after cycle B. Cycle A may cause greater expansion and contraction of the lattice with β–γ transformation than cycle B. After cycle A, the sample experiences larger lattice stress than that after cycle B. It seems likely that the protium concentration of β protide in the absorption–desorption cycle may cause a decrease of capacity and differently shaped PCT curves for cycles A and B.

Fig. 5 shows changes in the amount of desorption (a), the absorption and desorption pressure of the plateau (b), and mean particle size (c) versus the number of cycles. The open and closed circles (○ and ●) in the figure represent the absorption and desorption processes, respectively, after several repetitions of cycle A. The open and closed triangles (△ and ▲) represent the absorption and desorption processes, respectively, after several repetitions of cycle B. The amount of desorption is defined as the difference in the protium concentration at desorption between 7 and 0.01 MPa. The desorption and the mean particle size vary inversely with the logarithm of the cycle number up to 300 cycles. The particle size decreases from 1 to 2 mm before hydrogenation to less than 50 μm after the first cycle. Under cycle A conditions, the decrement of absorption pressure up to the 20th cycle is larger than that of desorption. To investigate the relationship between capacity and particle size, we determined the PCT curve of a sample with a mean particle size of about 13.8 μm (obtained by grinding under Ar). We found that the capacity does not directly depend on the particle size of the alloys.

Fig. 6 shows XRD patterns of the 40Ti–Cr–2.5Mo alloy after PCT measurement for several cycles. All samples contain about 0.5 H/M of residual protium after PCT measurement. All samples have only a β protide phase with a bcc structure. It was previously reported that the Ti–Cr–Mo alloys transform from the α phase as protium solid solutions with a bcc structure, via a β protide phase

APPENDIX 3

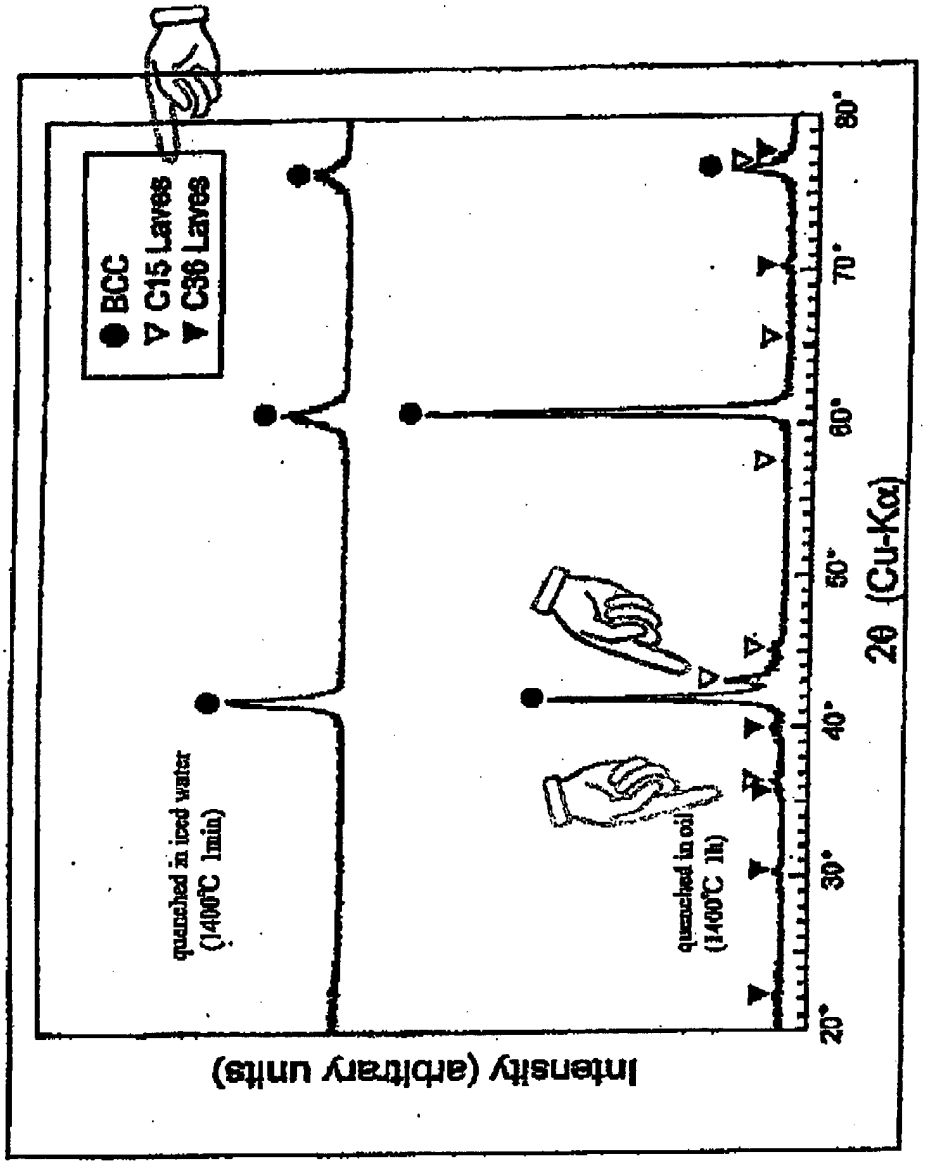

Graph.1
X-ray diffraction patterns of Ti-57.5Cr-2.5Mn alloys
(oil-quenched or iced water-quenched after heat treatment)

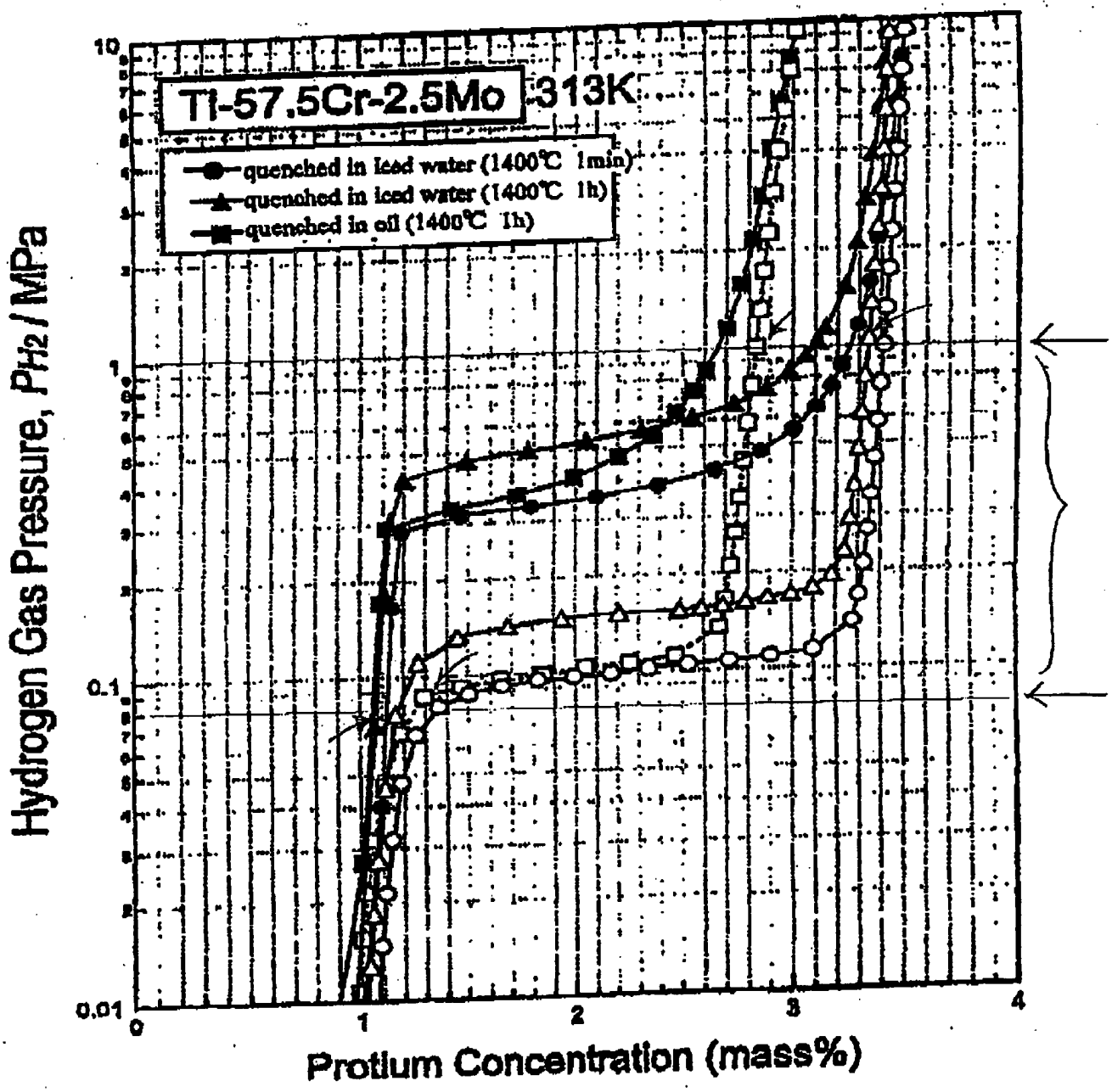

Graph.2
PTC curves of Ti-57.5Cr-2.5Mo alloys
(oil-quenched or iced water-quenched after heat treatment)

Ti-57.5 Cr-2.5 Mo alloy

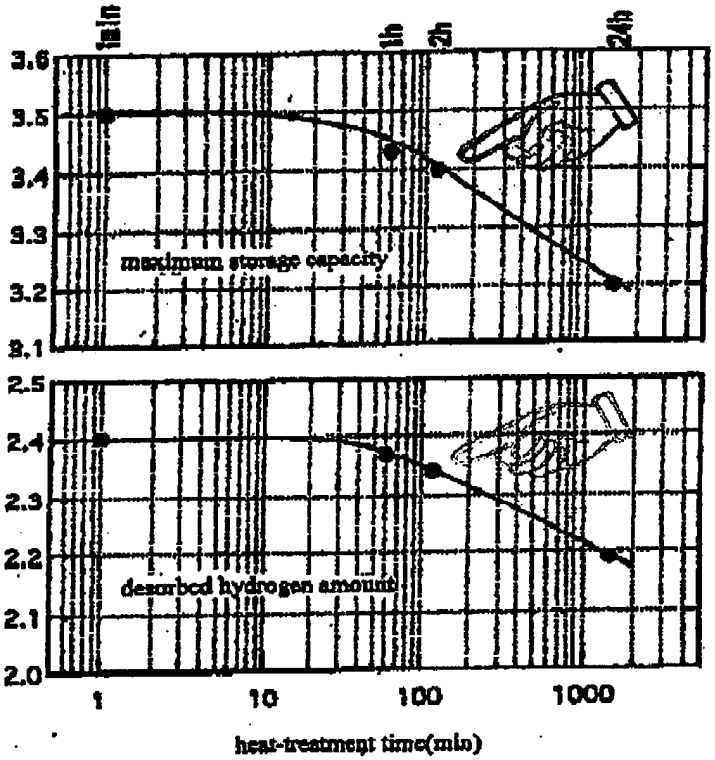

Graph.3
hydrogen absorption and desorption characteristics of
Ti-57.5 Cr-2.5 Mo alloy where the heat-treatment time varies at 1400°C

APPENDIX 4

Resume

Name: Masuo Okada
Date & July 5, 1948,
Place of Birth: Tochigi-Prefecture, Japan
Marirus Status: Married, Two children
Nationality: Japanese

Degrees:	Date	Institution
Bachelor of Science in Materials Science	March, 1971	Tohoku University
Master of Science in Materials Science	Sept., 1974	Univ. of California, Berkeley, U.S.A.
Master of Science in Materials Science Sendai, Japan	Sept., 1975	Tohoku University
Doctor of Philosopy in Materials Science	June, 1978	Univ. of California, Berkeley, U.S.A.

Thesis:

Ph.D Microstructure and Magnetic Properties of Spinodal Fe-Cr-Co alloys
Supervisor: Professor Gareth Thomas

Positions:

Research Associate: April 1979- November 1981
At the Department of Materials Science, Tohoku University, Sendai Japan 980
Associate Professor: November 1981- April 1993
ibid
Professor: May 1993-Present

Research Activities

Prof.Okada's research activities address new developments of a wide range of functional materials, such as hydrogen-absorbing materials, electroceramics, and magnetic materials.

Recently, he served as a leader of the Japanese national project "New Protium Function in Materials" to explore new, useful functions of the hydrogen atom in materials, with the budget of about 6.5million dollars, supported by the Japanese Ministry of Education, from 1998-2001. The project was finished with great success. The evaluation committee of the national project gave the highest evaluation of A to this project. One of the distinguished results was that Professor Okada successfully developed the Ti-Cr-V or Ti-Cr-Mo hydrogen absorbing alloys with 3mass% of hydrogen operated below 100°C, which is still world record up to now. He gave the invited talks on these Ti-Cr-V or Ti-Cr-Mo alloys at the International Symposium of Metal-Hydrogen, which is most prestigious international conference for hydrogen related materials, at Noosa in Australia on October of 2000, and at Annecy in France on September of 2002. . Because of his outstanding achievements in the field of developments of new hydrogen absorbing materials, he is regarded as one of the world's outstanding researchers in hydrogen societies.

Resume

Name: Takahiro Kuiiwa
Maritus Status: single
Nationality: Japanese

Degrees:	Date	Institution
Bachelor of Science in Materials Science	March, 1994	Tohoku University
Master of Science in Materials Science	March, 1997	Tohoku University
Doctor of Philosopy in Materials Science	March, 2000	Tohoku University Sendai, Japan

Thesis:

Ph.D Developments of V-based Hydrogen Absorbing Alloys with High Content of Hydrogen
Supervisor: Professor Masuo Okada

Positions:
Research Engineer
Engineering Research Department
Honda R&D Co.Ltd. Tochigi R&D Center
Tochigi, Japan

Individual Data

Name
OKADA Masuo

Affiliation
Graduate School of Engineering
Department of Materials Science

Title
Professor

Academic Degree
Ph.D

Academic Cluster

- MATERIALS CLUSTER
- EARTH AND ENVIRONMENT CLUSTER

Research Fields

- Functional Materials

Research Subjects

- Developmennt of new high density of Protium Alloys
- Syntheses of New Hydrides by Ultra-high Pressure
- Developments of new PTCR ceramics

Keywords
Hydrogen storage alloys, High-pressure hydrides, Grain-size refinement

Contributions to Publications

Ti-V-Cr b.c.c. alloys with high protium content.[Journal of Alloys and Compounds,330-331,(2002),511-516]M. Okada, T. Kuriiwa, T. Tamura, H. Takamura, A. Kamegawa

Protium absorption properties of Ti-V-Cr-Mn alloys with a b.c.c. structure.[Journal of Alloys and Compounds,330-332,(2002),522-525]T. Tamura, Y. Tominaga, K. Matsumoto, T. Fuda, T. Kuriiwa, A. Kamegawa, H. Takamura, M. Okada

Crystal structure of novel hydrides in a Mg-Ni-H system prepared under an ultra high pressure.[Journal of Alloys and Compounds,330-332,(2002),157-161]H. Takamura, H. Kakuta, A. Kamegawa, M. Okada

Web Site
http://ceram.material.tohoku.ac.jp/index-e.html

Updated on
2004.05.07

Top ▲

Special Functional Materilas Laboratory

Japanese version is here.


Masuo Okada, Prof.


Hitoshi Takamura Assoc. Prof.


Atsunori Kamegawa Research Assoc.

Research Topics

- ### Hydrogen Storage Materials

Hydrogen storage alloys, which can absorb and desorb hydrogen at room temperature, are promising candidates for use in fuel cell electric vehicles (FCEVs). In addition to the FCEVs, these alloys can be used in a variety of devices such as Ni-MH batteries and heat pumps. The storage capacity of these alloys is interestingly higher than that of pressurized gas cylinders and liquefied hydrogen, which are sometime troublesome to deal with. We are focusing on the development of high-performance hydrogen storage alloys, especially for Ti-based BCC alloys and Mg-based alloys.

- ### Ceramics Membranes for Hydrogen Production

To commercialize fuel cells for home use, it is required to develop hydrogen production technologies that can supply abundant high-purity hydrogen. Natural gas reforming is considered to be a most cost-effective and promising technique for hydrogen production. Instead of a steam reformer that have been well established, the purpose of this research project is to develop a high-performance natural gas reforming system, in which oxygen permeable ceramics and proton conductors are used for partial oxidation of methane and hydrogen separation, respectively. This system is expected to show higher efficiency compared to endothermic steam reformers. In addition to the high-performance oxygen permeable ceramics and proton conductors, the development of catalysts and thin-film fabrication techniques is also conducted in this research project.
More detailed information on this project can be found here.

- ### Grain size refinement for Mg-baed alloys by means of HDDR

Mg-based alloys have been used in a variety of industrial fields, including automobiles and mobile electronic devices, because of its lightweight and relatively high specific strength. However, the further improvement of mechanical properties and formability is required to enlarge the application fields. To do so, in addition to alloy development, the grain-size refinement is one of the most effective techniques. As a novel grain-size refinement technique, we are looking at the HDDR technology. The HDDR is the acronym of hydrogenation-disproportionation-desorption-recombination. This HDDR technique using heat treatment under hydrogen involves the disproportionation reaction along with the formation of hydrides followed by the recombination reaction resulting from the hydrogen desorption from the hydrides. The grain size of Mg-Al-based alloys subjected to this HDDR treatment, which is well know as AZ-series alloys and usually has a grain size of around 50~300 um, was found to be reduced down to 100 nm. We are further investigating the nature of the HDDR phenomena occurred in the Mg-Al-based alloys and to obtain finer grain sizes.